The Role of Ni-P Coating Structure on Fly Ash Cenospheres in the Formation of Magnesium Matrix Composites

KATARZYNA N. BRASZCZYŃSKA-MALIK and JACEK KAMIENIAK

The role of the Ni-P coating structure on fly ash cenospheres in the fabrication of magnesium matrix composites has been investigated. Two composites based on AZ91 commercial magnesium alloys with hollow aluminosilicate cenospheres were fabricated by the negative pressure infiltration technique. Two kinds of cenospheres (*i.e.*, as Ni-P coated and after heat treatment) were used in order to determine the influence of the Ni-P coating structure on creating interfaces between the components. Microstructure analyses were carried out by light microscopy, atomic force microscopy, XRD, scanning, and transmission electron microscopy. Al_3Ni_2 and Mg_2Ni intermetallic phases at the component interfaces were formed in the composite with as-received Ni-P-coated cenospheres. After heat treatment of the Ni-P-coated cenospheres, NiO was created outside the external layer of the Ni-P coatings and this oxide remained stable at the component interfaces during composite fabrication. In both cases, the Ni-P coating prevented the reaction between the cenosphere walls and the magnesium matrix alloy, which contributed to obtaining intact cenospheres, unfilled by the matrix alloy.

DOI: 10.1007/s11661-017-4272-x

I. INTRODUCTION

METAL matrix composites reinforced with different fibers or ceramic particles deserve special consideration due to their properties, especially low density, high specific stiffness and strength, high damping capacity, and good dimension stability.[1–3] What is more, metal matrix composites based on different matrix alloys with fly ash cenospheres are materials that have recently been intensively investigated.[4–6] Cenospheres (also called microballoons) are thin-walled, hollow, ceramic particles of different sizes (up to 500 μm) and a very low true density equal to about 0.4 to 0.6 g/cm^3. The cenosphere walls belong to glass ceramic materials based on aluminosilicate glass, mullite, quartz, calcite, iron oxides, and calcium silicates and sulfates.[7–9] The wall thickness of cenospheres is generally 5 to 10 pct of that of their diameter, whereas the glassy phase content in the wall material is about 80 to 90 pct. Hollow cenospheres are filled with gases like CO_2 and N_2 with traces of CO, O_2, and H_2O. It should also be noted that cenospheres as a by-product of coal-fired power plants could contribute to reducing the cost of metal matrix composites.[10,11]

In recent years metal matrix composites based on magnesium alloys with cenospheres have also been synthesized.[12–15] Magnesium alloys are light metallic structural materials and have a unique combination of properties, which are very attractive in such applications as the automotive, aerospace, and electronic industries.[15–17] Therefore, these alloys are attractive as a composite matrix. Rohatgi *et al.*[18] obtained by the die casting technique a composite based on the AZ91 magnesium alloy matrix with cenospheres. Analogical material was fabricated by the stir casting method by Huang *et al.*,[19] Lu *et al.*,[20] and Gupta *et al.*[21] A composite based on the AZ91 alloy with cenospheres was obtained by the pressure infiltration process by Liu *et al.*[22] Daoud *et al.*[23] investigated a composite fabricated on the base of the ZC63 magnesium alloy by the stir casting technique. The main problem during the fabrication of cast metal matrix composites with cenospheres is the destruction of their walls due to mechanical damage or chemical reaction with the liquid alloy matrix.[1–4,12] During the processes of composite fabrication like stir casting, die casting, or pressure infiltration method, thin-walled, hollow cenospheres could easily undergo damage due to mixing or pressure actions. On the other hand, magnesium alloys (due to their high reactivity) are especially prone to reactions with the oxides forming the cenosphere walls. In consequence, the obtained composites are characterized

KATARZYNA N. BRASZCZYŃSKA-MALIK and JACEK KAMIENIAK are with the Institute of Materials Engineering, Czestochowa University of Technology, Al. Armii Krajowej 19, 42-200 Czestochowa, Poland. Contact e-mail: kacha@wip.pcz.pl
Manuscript submitted November 21, 2016.
Article published online September 19, 2017

by a majority or part the cenospheres broken and filled by the matrix alloy. The main reaction products between the components in magnesium matrix composites with fly ash cenospheres are the Mg_2Si phase and MgO.[12–14] It should be noted that generally reactions occurring in many metal/ceramic systems may either cause the formation of transitional layers at the component interfaces or/and significantly change the phase composition of the matrix alloy. The especially large Mg_2Si phase formed with blocky morphology in the described composites with aluminosilicate cenospheres was located both at the component interfaces and within the matrix alloy. An analogical situation was observed in different composites, for example, fabricated on the base of a magnesium alloy with rare earth elements (RE). Introducing SiC particles into the Mg-RE alloy caused changes in the matrix composition, creating an RE_3Si_2 phase located both within the matrix alloy and at the component interfaces due to reaction between the reinforced particles and alloying elements.[24] Similar to composites fabricated on the base of Mg, some content of SiO_2 on the SiC particles caused the creation of an Mg_2Si phase located both at the component interfaces and in the matrix alloy.[25]

One of the methods of preventing undesirable reactions between the components in metal matrix composites is to coat the reinforcing phases. Daoud *et al.*[4] applied nickel-coated fly ash microballoons as fillers of a composite based on a Pb-Ca-Sn alloy fabricated by the stir casting method. They did not reveal significant reactions occurring at the interfaces between the cenospheres and the Pb alloy matrix. Ni coatings were also applied on different reinforcing phases in order to obtain wettability or prevent reactions between the components.

In the present work, a magnesium matrix composite with Ni-P-coated cenospheres is presented. The experimental composite was fabricated by the negative pressure infiltration method. The microstructure investigations and analysis of the interfaces between the components were carried out in order to describe the role of the Ni-P coating structure in preventing reactions between the cenosphere walls and the liquid magnesium alloy matrix.

II. MATERIALS AND EXPERIMENTAL PROCEDURES

The commercial AZ91 magnesium alloy was used as the matrix alloy with the chemical composition specified by ASTM B93-94: 9 wt pct Al, 0.9 wt pct Zn, and 0.4 wt pct Mn. The as-received hollow aluminosilicate cenospheres with a particle size distribution varying from 63 to 125 μm were supplied by the Opole (Poland) electric power station. The chemical composition was as follows: 53 to 63 wt pct SiO_2, 21 to 31 wt pct Al_2O_3, 4.4 to 5.6 wt pct Fe_2O_3, 1.5 to 2.5 wt pct CaO, 0.3 to 0.7 wt pct MgO, 0.8 to 1.6 wt pct $K_2O + Na_2O$, and 0.1 to 0.7 wt pct TiO_2. The Ni-P coating on the cenospheres was performed by the electroless plating method described in work.[26] The thickness of the obtained

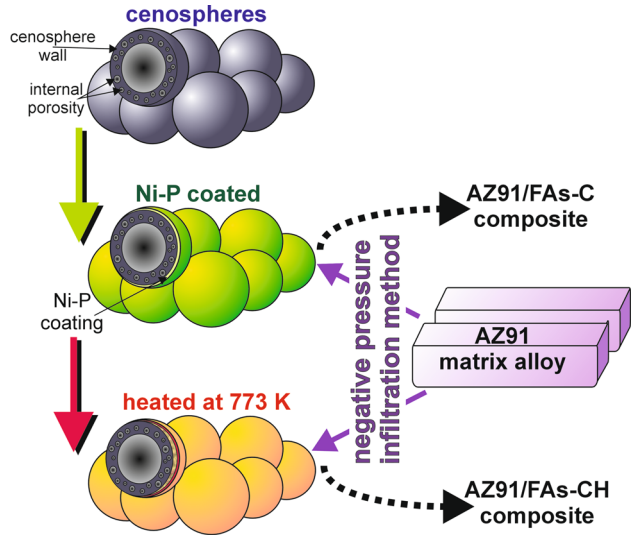

Fig. 1—Scheme of component preparation method.

Ni-P layer on the cenospheres was equal to about 0.4 μm. The cenospheres were used just after the coating process (composite named AZ91/FAs-C in this work) and after heat treatment of the Ni-P coated material at 773 K (500 °C) (composite named AZ91/FAs-CH). Figure 1 shows the scheme of the component preparation. The composite was fabricated by the negative pressure infiltration method.[27] In both cases, the steel mold was initially heated up to 773 K (500 °C). The volume fraction of the cenospheres in the fabricated composites was verified by the linear method.

The phase compositions of the investigated materials (coated cenospheres and composites) were analyzed by the X-ray diffraction (XRD) method using a Bruker D8 ADVANCE diffractometer. $Cu_{K\alpha}$ X-ray radiation was used with an angular step equal to 0.02 deg. Reflexes from particular phases were identified according to ICDD PDF-4+ cards.[28] The Ni-P coating on the cenospheres was also examined by an Veeco atomic force microscope (AFM) with the tapping mode procedure. The NanoScope 7.20 program was used to determine the surface roughness parameters of the Ni-P coating like R_a (Center Line Average High) and SAD (Surface Area Difference). Analyses were performed on areas equal to 0.04 μm.

The composite specimens for the microstructure investigations were prepared by standard metallographic procedures including wet prepolishing and polishing with different diamond pastes without contact with water. To reveal the matrix alloy microstructure, the samples were etched in a 1 pct solution of HNO_3 in C_2H_5OH. The microstructure examinations were performed by an Olympus GX51 light microscope (LM) with differential-interfaces contrast (DIC) and a JOEL JSM-6610LV scanning electron microscope with an energy dispersive X-ray spectrometer (SEM + EDX). The microstructure of the interfaces between the components was also examined by transmission electron microscopy (TEM). A TECAI G^2 FEG transmission electron microscope with EDAX equipment was used.

The samples for the TEM investigations were cut in the form of 3 mm discs. They were next dimpled and mechanically thinned using a Gatan 656 dimple and finally thinned using Leica-EM RES 101 equipment. Brightfield and darkfield techniques were used for the microstructure observations and selected area electron diffraction (SAED) patterns were employed to define the structural constituents.

III. RESULTS AND DISCUSSION

Figure 2 shows the images of the used cenospheres with the Ni-P coating. It can be seen that the morphology of the used cenospheres reveals a spherical shape with a generally smooth exterior surface. The obtained Ni-P coating had about an 0.4 μm thickness, which is clearly visible especially on the plane perpendicular to the cenosphere walls (on the fracture surface) shown in Figure 2(c). The coating had a permanent structure and it was closely connected with the cenospheres. The Ni-P-coated cenospheres were heat treated at 773 K (500 °C). Heating at this temperature did not cause defects in the Ni-P coating like cracking or chipping. Figure 3 presents a comparison of the surface topography of the Ni-P coating after electroless plating (Figures 3(a) and (c)) and heat treatment at 773 K (500 °C) (Figures 3(b) and (d)), obtained by the AFM technique. Heat treatment caused a slight rise in the R_a parameter from 5.05 nm for the surface of the Ni-P coating to 5.15 nm for the heated material. The SAD parameter also increased from 16.40 to 16.93 after heat treatment of the Ni-P coating.

Figure 4 shows the X-ray diffraction micrographs of both types of used cenospheres. They confirmed that the used cenospheres are mainly composed of mullite and quartz. The broad diffraction reflexes also indicate the presence of an amorphous (glass) phase in the cenosphere walls. It should be noted that the applied heat treatment of the Ni-P-coated cenospheres caused differences in the phase composition of the Ni-P coating. The Ni-P coating on the cenospheres performed by the electroless plating method had an amorphous structure, which is revealed by the broad diffraction reflex from nickel (Figure 4(a)). The heat treatment of the cenospheres at 773 K (500 °C) caused the Ni and Ni_3P phases inside the coating to crystallize. The sharp deflection reflexes visible in Figure 4(b) clearly disclosed the presence of those crystalline phases in the Ni-P coating. Additionally, the X-ray analyses also revealed a significant presence of reflexes from the NiO phase. Because the heat treatment process was conducted in air, an NiO layer was formed on the Ni-P coating due to the oxidation reaction. The reason for the Formation of this oxide was the increase in the above-described surface roughness parameters, determined by the AFM technique.

Figures 5 and 6 present microstructure images of the composites fabricated with as-received Ni-P-coated cenospheres (composite AZ91/FAs-C) and after heat treatment (AZ91/FAs-CH), respectively. In both cases, hollow cenospheres were successfully incorporated into

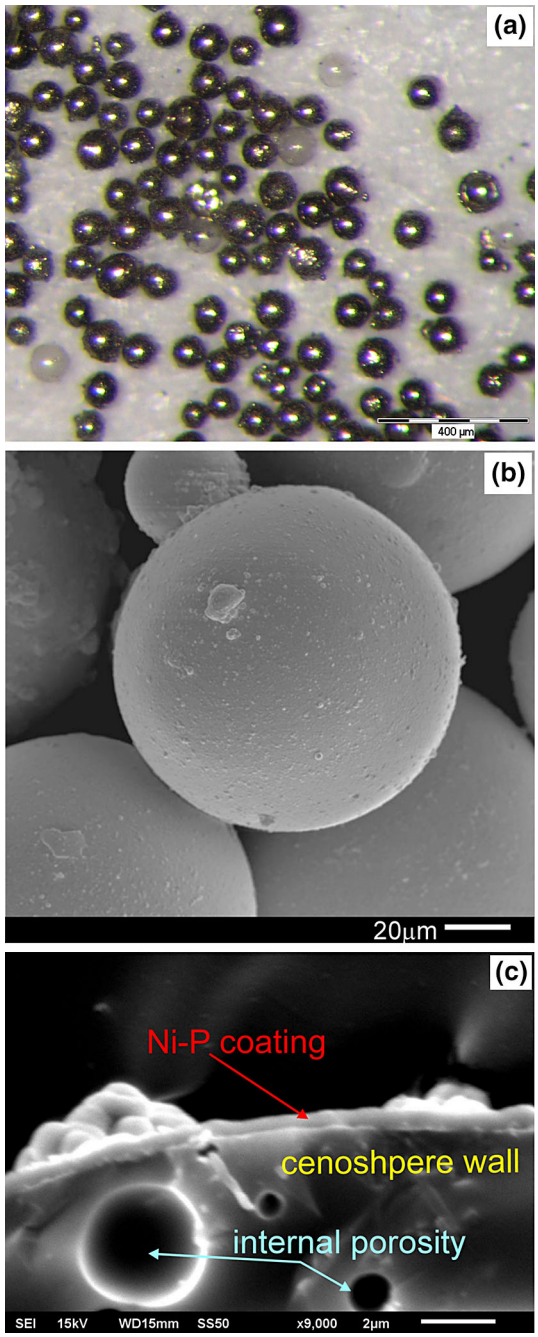

Fig. 2—LM (*a*) and SEM (*b*) images of Ni-P coated fly ash cenospheres. Transverse section of Ni-P coating cenosphere wall (fracture surface); SEM (*c*).

the matrix alloy. It should be noted that both the investigated composites were characterized by uniform distribution of intact cenospheres unfilled by the matrix alloy. In addition, in both cases the volume fraction of the cenospheres was about 60 vol pct. The presented composites' microstructure with cenospheres unfilled by the matrix alloy was a consequence of both the used Ni-P-coated cenospheres and the negative pressure infiltration method for composite fabrication. The relatively low pressure used during this method of composite fabrication did not cause cenosphere damage.

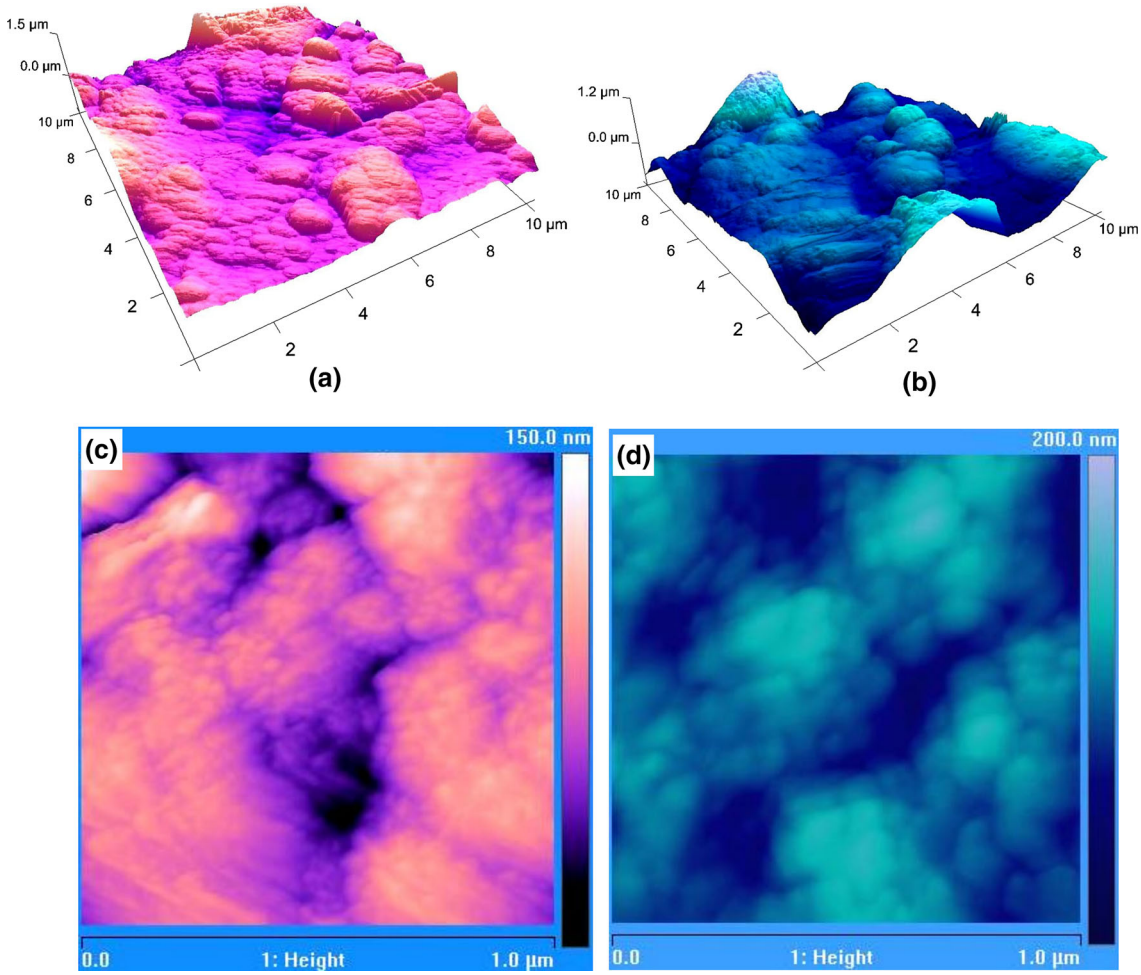

Fig. 3—AMF images showing surface topography 3D (*a*, *b*) and 2D (*c*, *d*) of Ni-P coated (a, c) and heat treated at 773 K (500 °C) (b, d) cenospheres.

Nevertheless, the composite with the as-received Ni-P-coated cenospheres (AZ91/FAs-C) was characterized by visible porosity between the cenospheres. Figure 5 shows the microstructure of this composite where entrapped air porosity in the matrix alloy was observed in the region between the hollow cenospheres. Although the steel mold was heated up to 773 K (500 °C), using cold cenospheres hampered the molten matrix stream by crystallizing phases. Analogical porosity was also observed by Rohatgi *et al.*[6] in the microstructure of A356/fly ash cenosphere syntactic foam. In the case of the AZ91/FAs-CH composite, both hot cenospheres and mold enabled filling of all the spaces between the cenospheres by the molten alloy matrix (Figure 6). This material was free from porosity or other casting defects.

For both composites, the microstructure of the matrix alloy had a dendritic morphology with very strong segregation of the alloying element, typical for cast AZ91 alloy. The microstructure consisted of a hexagonal closely packed α-Mg solid solution dendrite, depleted in alloying elements in comparison to the equilibrium conditions and $\alpha + \gamma$ divorced eutectic. In Mg-Al-type alloys the γ-phase (called also β-phase) is an intermetallic compound with a stoichiometric composition of $Mg_{17}Al_{12}$ (at 43.95 wt pct Al) and an α-Mn-type cubic unit cell. Due to the presence of zinc in the chemical composition of the AZ91 alloy, a ternary intermetallic compound $Mg_{17}Al_{11.5}Zn_{0.5}$ or $Mg_{17}(Al,Zn)_{12}$ type was created because zinc substitutes aluminum in the γ phase.[29,30] Additionally, the γ phase in the form of secondary discontinuous precipitates was revealed in the microstructure of both fabricated composites. A characteristic lamellar structure with a marked anisotropy of growth of a plate-like γ phase, located especially near the $\alpha + \gamma$ eutectic was visible in the microstructure of both composites (Figures 5 and 6). Discontinuous precipitates of the γ phase were formed from the solid state below the solvus temperature. This precipitation process is the cellular growth of alternating plates of the secondary phase and near-equilibrium matrix phase. This structural constituent is typical for AZ91 alloy solidified especially in a sand mold where the cooling rate of the cast is relatively slow.[31] In the presented case, due to the high temperature of the steel mold [773 K (500 °C)] the solidified composites cooled down sufficient slowly so that the precipitation process could take place.

Additionally, it should be noted that differences in the cenosphere/matrix interface morphology were revealed

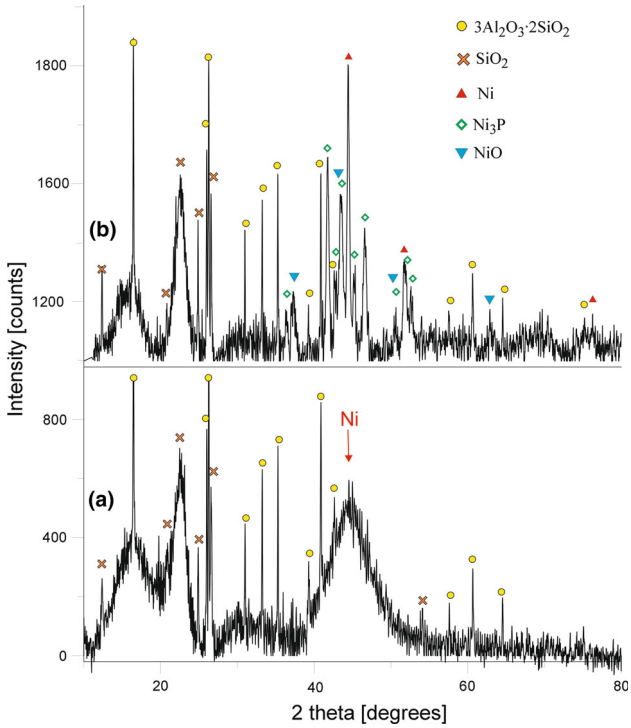

Fig. 4—X-ray diffraction pattern of Ni-P coated (*a*) and heat treated at 773 K (500 °C) (*b*) cenospheres.

during microstructure observation. In the case of the AZ91/FAs-C composite, fine phases with blocky morphology were observed at the cenosphere/matrix alloy interfaces. Figures 5(c) and (d) illustrate very distinct phases created at the external walls of the cenospheres. The observed fine phases at the component interfaces testify to the reaction between the Ni-P coating and the AZ91 magnesium alloy matrix. According to Thermo-Calc software (Stockholm, Sweden) data, the possible reaction products that can form at the cenospheres/matrix alloy interface in the AZ91/FAs-C composite are Al_3Ni_2, Al_3Ni, $AlNi_3$, AlNi, $MgNi_2$, and Mg_2Ni. It should be noted that on the contrary in the case of the AZ91/FAs-CH composite, the interfaces between components were smooth. Differences in the interface structure morphology for both the investigated composites are clearly visible from comparison Figures 5 and 6.

The presence of the observed structural constituents was confirmed by X-ray analyses. Figure 7 presents X-ray diffraction micrographs of the investigated materials. It was revealed that for both composites the matrix alloy was composed of an α-Mg and γ phase. Additionally, reflexes coming from phases disclosed for the cenospheres (presented in Figure 4), like mullite and quartz, were also distinct in the X-ray diffraction patterns obtained from both the composites. The high volume fraction of the cenospheres influenced the intensity of those reflexes. It should be noted that the

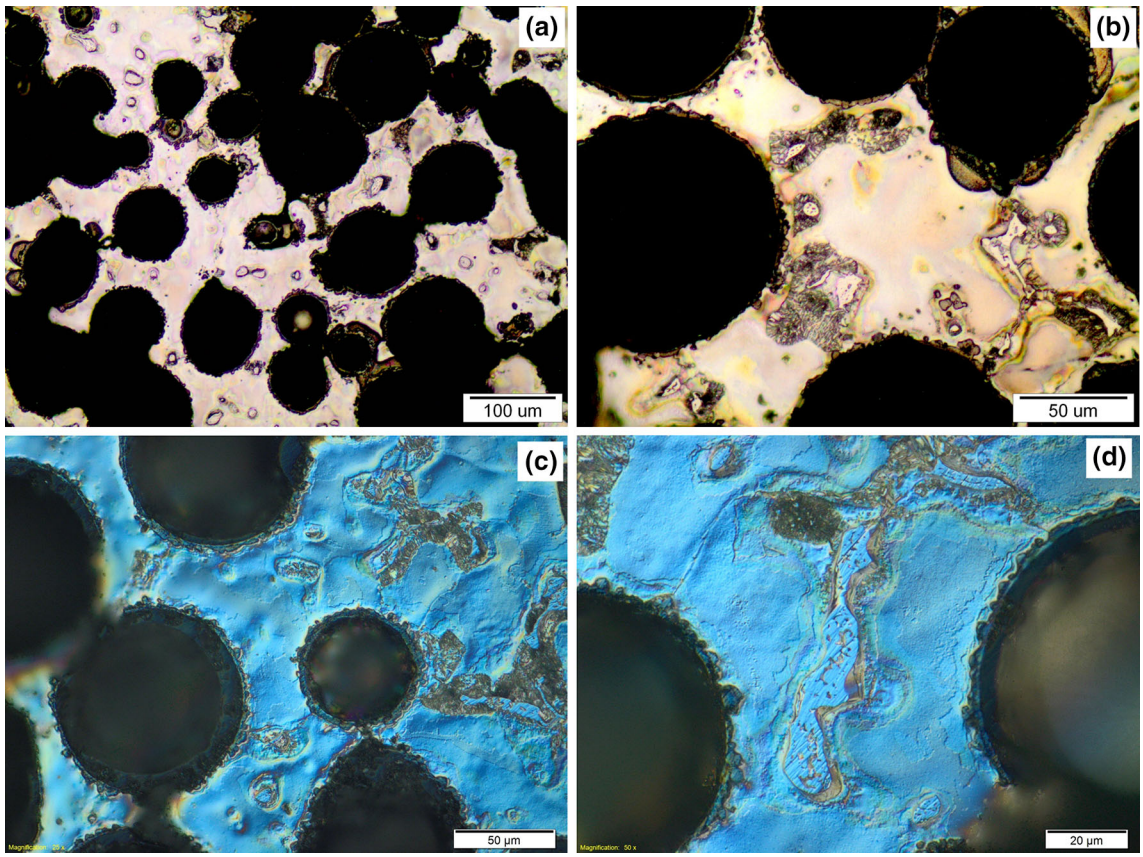

Fig. 5—Microstructure of AZ91/FAs-C composite (LM-DIC).

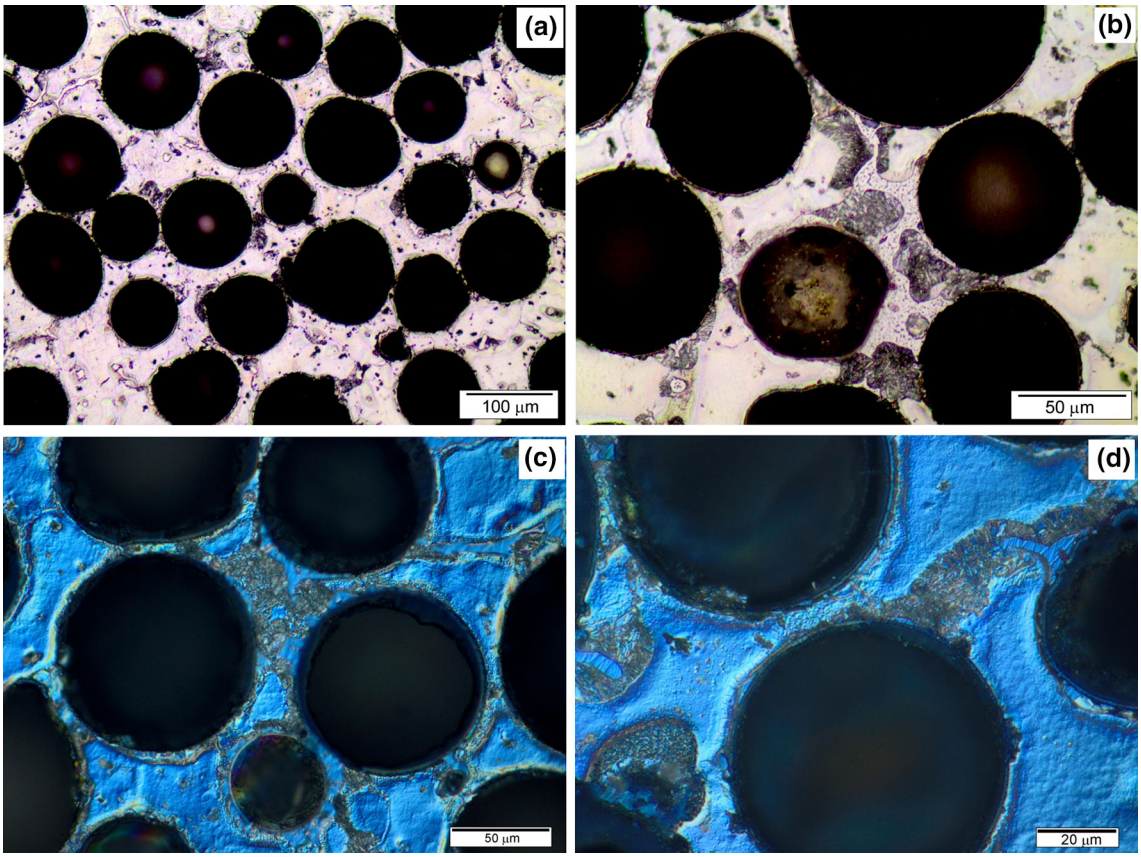

Fig. 6—Microstructure of AZ91/FAs-CH composite (LM-DIC).

X-ray analyses also revealed the differences in the phase composition of the fabricated materials. For the AZ91/FAs-C composite, reflexes from the Al_3Ni_2 and Mg_2Ni intermetallic phases were identified (Figure 7(a)), whereas these structural constituents were not present on the X-ray diffraction pattern obtained from the AZ91/FAs-CH composite. On the other hand, the X-ray analyses of the AZ91/FAs-CH composite revealed a significant presence of Ni, Ni_3P, and NiO phases (Figure 7(b)). It should be noted that reflexes from the NiO were not disclosed during analyses of the AZ91/FAs-C composite. The microstructure of the AZ91/FAs-C composite was also observed by the scanning electron microscope. EDX line measurements were performed on polished specimens perpendicular to the interface layer between the cenospheres and matrix alloy for a total length of about 40 μm. The SEM + EDX results presented in Figure 8 allowed the authors to confirm the presence of Al_3Ni_2 and Mg_2Ni intermetallic phases at the cenosphere/matrix alloy interfaces in this composite. Linear distribution of the elements along the line cutting across the interface between the components displayed a significantly increased content of Al and Ni in one area and a raised Mg and Ni content in the other side. It should also be noted that a raised Ni content was continuous outside the cenosphere wall. On the other hand, the content of oxygen was significantly increased only in the cenosphere wall. The results obtained from SEM + EDX analyses (Figure 8) in combination with

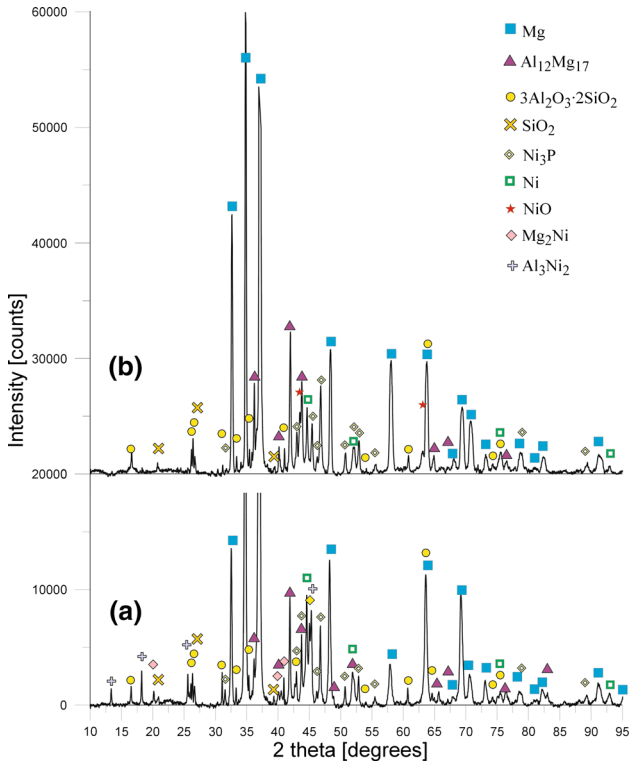

Fig. 7—X-ray diffraction pattern of AZ91/FAs-C (*a*) and AZ91/FAs-CH (*b*) composites.

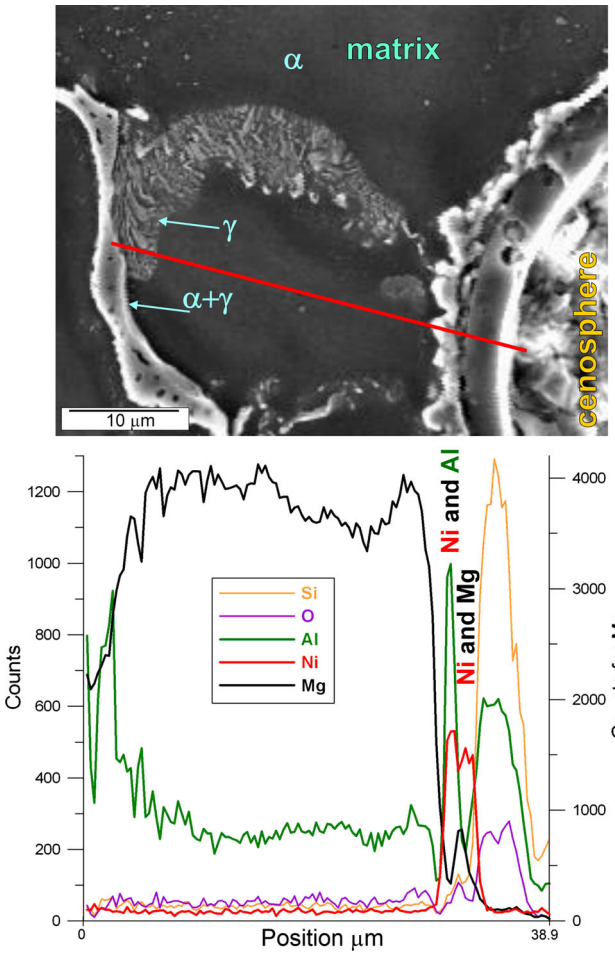

Fig. 8—SEM image of AZ91/FAs-C composite microstructure with EDX results.

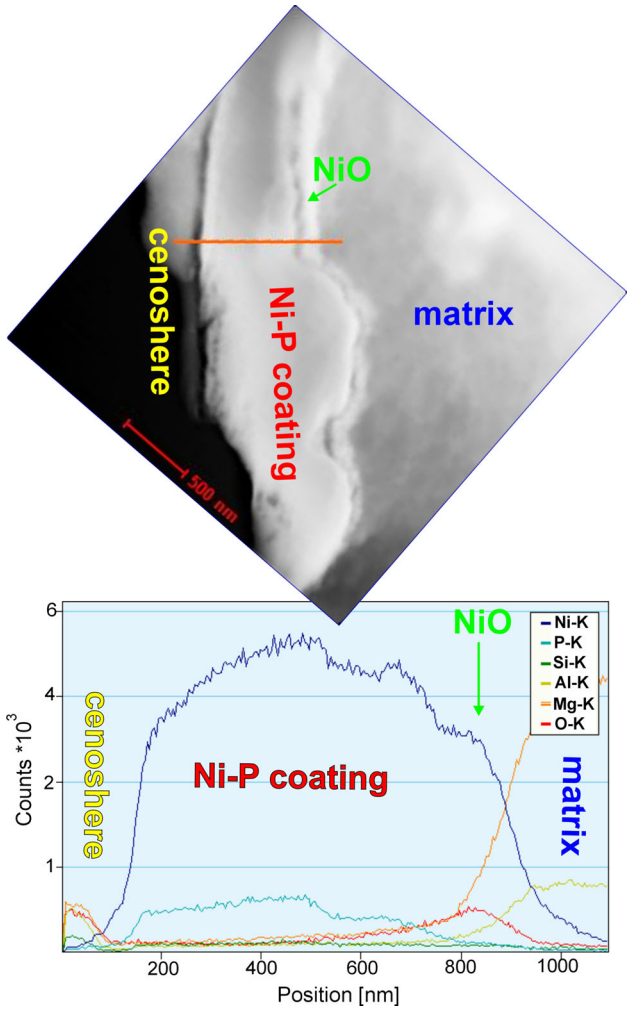

Fig. 9—TEM image of AZ91/FAs-CH composite with EDAX results.

the results acquired from the X-ray analyses (Figure 7(a)) testified that at the cenosphere/matrix alloy interfaces Al_3Ni_2 and Mg_2Ni intermetallic phases were formed. The above phases were formed due to the reaction between the Ni-P coating and liquid alloy matrix during the AZ91/FAs-C composite fabrication process. Although the reaction time between the Ni-P coating and the molten alloy matrix during fabrication was relatively short, especially in the case of the used cenospheres at ambient temperature, the presence of Al_3Ni_2 and Mg_2Ni phases in the investigated AZ91/FAs-C composite microstructure was demonstrated. Leon-Patiño *et al.*[32,33] also revealed an Al_3Ni_2 phase in aluminum matrix composites reinforced with Ni-P-coated SiC particles fabricated by the infiltration method. On the other hand, an Mg_2Ni phase was also observed by Hassan *et al.*[34] in an Mg-Ni composite and by Tsai *et al.*[35] in the Mg-Ni system.

The cenosphere/matrix alloy interfaces in the AZ91/FAs-CH composite were investigated by the TEM technique. TEM observations clearly confirmed the presence of Ni-P coating on the cenospheres. Figure 9 shows a TEM image of the Ni-P coating on a fly ash cenosphere in contact with the matrix alloy. Additionally, the thin permanent external layer of the Ni-P coating located on the matrix side is visible. The linear distribution of elements along the line cutting across the interface between the components displayed a significant increase in Ni and P content in the coating and raised oxygen content in the external layer of the Ni-P coating (on the matrix side). The increased content of oxygen testified to the presence of NiO, which was confirmed by SAED analyses.

Figure 10 presents the TEM image of the interface between the components with SAED patterns obtained from different places of the observed Ni-P coating and EDAX results of surface distribution of elements obtained from the marked area. The associated SAED pattern obtained from the external layer of the Ni-P coating confirmed the identification of the NiO phase. The presence of NiO at the Ni-P coating external layer was also confirmed by the surface distribution of elements revealed during TEM + EDAX analyses presented in Figure 10. On the other hand, the associated SAED patterns obtained from different places of the Ni-P coating revealed the presence of both Ni_3P and Ni phases inside the coating. It should also be noted that

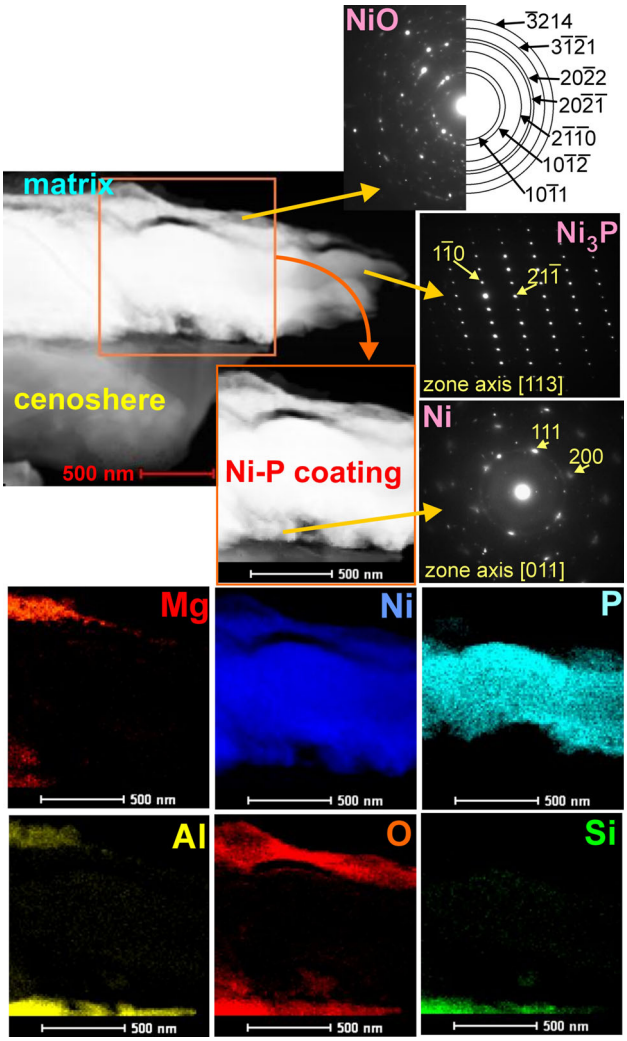

Fig. 10—TEM images of AZ91/FAs-CH composite with EDAX results and diffraction patterns obtained from observed structural constituents.

that rings visible on the diffractions received from both NiO and Ni testified to the fine-crystalline structure of these phases. The above phases identified during TEM analyses of the fabricated AZ91/FAs-CH composite were also revealed during X-ray analyses of the Ni-P-coated cenospheres heated to 773 K (500 °C) (Figure 4(b)). It should be noted that MgO which potentially can be created was not revealed during TEM analyses. Although the NiO external layer on Ni-P coating is potentially prone to reduction by the liquid magnesium to form MgO, the short time of the infiltration method nevertheless precluded reaction between components.

The presented investigation results indicated that structure of the Ni-P coating had an influence on the interface boundary between the components in magnesium matrix composites with cenospheres. Ni-P coating with amorphous structure as-received from the electroless plating method was prone to reaction with the liquid AZ91 magnesium alloy matrix. The Al_3Ni_2 and Mg_2Ni reaction products created during AZ91/FAs-C composite fabrication were located at the external layer of the Ni-P coating in the form of blocky phases visible in Figures 5 and 8. Although the reaction between the Ni-P coating and matrix alloy took place, the layers of the Ni-P coat and Al_3Ni_2 and Mg_2Ni intermetallic phases prevented the reactions between the cenospheres and the AZ91 alloy. A different interface structure was obtained during AZ91/FAs-CH composite fabrication. The heat treatment of the Ni-P-coated cenospheres caused crystallization of the Ni_3P and Ni phases inside the coating and creation of an NiO layer at its external layer. Those phases were stable during the composite fabrication process and formed perpetual layers on the cenosphere walls. The presented results unequivocally proved that this Ni-P coating prevents component reactions. Both types of component interfaces obtained during fabrication of the investigated composites are presented schematically in Figure 11. It should be noted that despite obtaining different interface structures

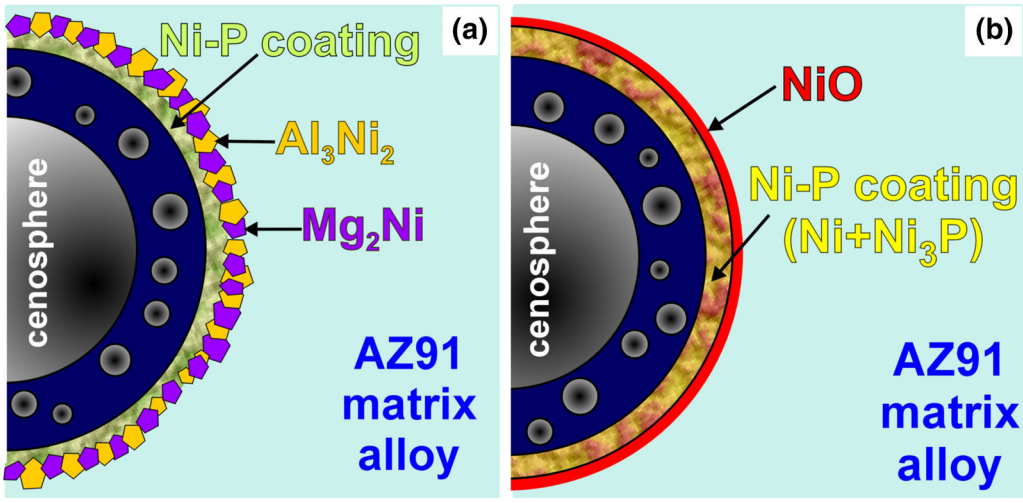

Fig. 11—Schemes of interfaces between components in investigated AZ91/FAs-C (*a*) and AZ91/FAs-CH (*b*) composites.

between the cenospheres and AZ91 magnesium alloy, both types protected the cenospheres from reactions with the liquid alloy matrix.

IV. CONCLUSIONS

The fabricated composites were characterized by uniform distribution of Ni-P-coated cenospheres unfilled by the AZ91 magnesium alloy. The structure of the Ni-P coating on the cenospheres had an influence on their behavior during composite fabrication. The as-received Ni-P coating reacted with the molten AZ91 alloy matrix to form Al_3Ni_2 and Mg_2Ni intermetallic phases at the component interfaces. Heat treatment of the Ni-P coating resulted in the formation Ni_3P and Ni phases inside the coating and the creation of NiO layer at its external layer. Those phases were stable during the composite fabrication process. Both types of interfaces between the components effectively prevent the reactions between the cenosphere walls and the magnesium alloy matrix.

OPEN ACCESS

REFERENCES

1. Y. Lin, Q. Zhang, and G. Wu: *J. Alloys Compd.*, 2016, vol. 655, pp. 301–08.
2. D.P. Mondal, J.D. Majumder, N. Jha, A. Badkul, S. Das, A. Patel, and G. Gupta: *Mater. Des.*, 2012, vol. 34, pp. 82–89.
3. C.A. Vogiatzis and S.M. Skolianos: *Compos. Part A*, 2016, vol. 82, pp. 8–19.
4. A. Daoud, M.T. Abou Al-Khair, A.Y. Shenouda, and P.K. Rohatgi: *Mater. Sci. Eng. A*, 2009, vol. 526, pp. 225–34.
5. I.N. Orbulov and J. Ginsztler: *Compos. Part A*, 2012, vol. 4, pp. 553–61.
6. P.K. Rohatgi, N. Gupta, B.F. Schultz, and D.D. Luong: *JOM*, 2011, vol. 63, pp. 36–42.
7. A.V. Vassilev, R. Menedez, D. Alvarez, M. Diaz-Somoano, and M.R. Martinez-Tarazona: *Fuel*, 2003, vol. 82, pp. 1793–1811.
8. A.V. Vassilev, R. Menedez, D. Alvarez, M. Diaz-Somoano, and M.R. Martinez-Tarazona: *Fuel*, 2004, vol. 83, pp. 585–603.
9. B.G. Kutchko and A.G. Kim: *Fuel*, 2006, vol. 85, pp. 2537–44.
10. W. Pichór, K. Mars, E. Godlewska, and R. Mania: *Kompozyty (Composites)*, 2010, vol. 10, pp. 149–53.
11. T. Matsunaga, J.K. Kim, S. Hardcastle, and P.K. Rohatgi: *Mater. Sci. Eng. A*, 2002, vol. A325, pp. 333–43.
12. Z. Huang, S. Yu, J. Liu, and X. Zhu: *Mater. Des.*, 2011, vol. 32, pp. 4714–19.
13. Z. Huang and S. Yu: *J. Alloys Compd.*, 2010, vol. 509, pp. 311–15.
14. J. Kamieniak and K.N. Braszczynska-Malik: *Compos. Theory Pract.*, 2014, vol. 14, pp. 214–18.
15. P.K. Rohatgi, J.K. Kim, N. Gupta, S. Alaraj, and A. Daoud: *Compos. Part A*, 2006, vol. 37, pp. 430–37.
16. D.D. Luong, N. Gupta, and P.K. Rohatgi: *JOM*, 2011, vol. 63, pp. 48–52.
17. S.R. Yu and Z.Q. Huang: *J. Mater. Eng. Perform.*, 2014, vol. 23, pp. 3480–88.
18. P.K. Rohatgi, A. Daoud, B.F. Schultz, and T. Puri: *Compos. Part A*, 2009, vol. 40, pp. 883–96.
19. Z. Huang, S. Yu, and M. Li: *Trans. Nonferrous Met. Soc. China*, 2010, vol. 20, pp. 458–62.
20. N.N. Lu, X.J. Wang, L.L. Meng, C. Ding, W.Q. Liu, H.L. Shi, X.S. Hu, and K. Wu: *J. Alloys Compd.*, 2015, vol. 650, pp. 871–77.
21. N. Gupta, D.D. Luong, and K. Cho: *Metals*, 2012, vol. 2, pp. 238–52.
22. J.A. Liu, S.R. Yu, Q. Huang, G. Ma, and Y. Liu: *J. Alloys Compd.*, 2012, vol. 537, pp. 12–18.
23. A. Daoud, M.T. Abou El-Khair, M. Abdel-Aziz, and P. Rohatgi: *Comp. Sci. Technol.*, 2007, vol. 67, pp. 1842–53.
24. K.N. Braszczyńska: *Zeitsch. Metallkunde*, 2003, vol. 94, pp. 144–48.
25. K.N. Braszczyńska and A. Bochenek: *La Rev. Metal.*, 2000, vol. 97, pp. 1455–62.
26. J. Kamieniak: AZ91 magnesium matrix composites with aluminosilicate cenospheres, Doctoral Thesis, Czestochowa University of Technology, Czestochowa 2012.
27. J. Kamieniak., K. Braszczynska-Malik: Method for producing a composite material of metal ceramic compound particles, Patent PL400705(A1).
28. Powder Diffraction File, PDF-4+ 2014, International Centre for Diffraction Data (ICDD), Pennsylvania, USA.
29. K.N. Braszczyńska-Malik and M. Mróz: *J. Alloys Compd.*, 2011, vol. 609, pp. 9951–58.
30. K.N. Braszczyńska, L. Lityńska, and W. Baliga: *J. Micros.*, 2006, vol. 224, pp. 15–17.
31. K.N. Braszczyńska-Malik: in *Magnesium alloys—design, processing and properties*, Czerwinski F, ed., INTECH Open Access Publisher, 2011, Chap. 5. pp. 95–112.
32. C.A. Leon-Patiño and R.A. Drew: *Current Opin. Solid State Mater. Sci.*, 2005, vol. 9, pp. 211–18.
33. C.A. Leon and R.A. Drew: *Compos. Part A*, 2002, vol. 33, pp. 1429–32.
34. S.F. Hassan and N. Gupta: *J. Alloys Compd.*, 2002, vol. 335, pp. 10–15.
35. M.Y. Tsai, M.H. Chou, and C.R. Kao: *J. Alloys Compd.*, 2009, vol. 471, pp. 90–92.